



Published in final edited form as:

Nat Neurosci. 2019 September ; 22(9): 1383–1388. doi:10.1038/s41593-019-0455-7.

RPS25 is required for efficient RAN translation of *C9orf72* and other neurodegenerative disease-associated nucleotide repeats

Shizuka B. Yamada^{1,2}, Tania F. Gendron³, Teresa Niccoli^{4,7,8}, Naomi R. Genuth^{1,2,5}, Rosslyn Grosely⁶, Yingxiao Shi⁹, Idoia Glaria^{4,7}, Nicholas J. Kramer^{1,10}, Lisa Nakayama¹, Shirleen Fang¹, Tai J. I. Dinger^{1,2}, Annora Thoeng^{4,7,8}, Gabriel Rocha⁹, Maria Barna^{1,5}, Joseph D. Puglisi⁶, Linda Partridge⁸, Justin K. Ichida⁹, Adrian M. Isaacs^{4,7}, Leonard Petrucelli³, Aaron D. Gitler^{1,11}

¹ Department of Genetics, Stanford University School of Medicine, Stanford, CA USA

² Department of Biology, Stanford University, Stanford, CA USA

³ Department of Neuroscience, Mayo Clinic, Jacksonville, FL USA

⁴ Department of Neurodegenerative Disease, UCL Institute of Neurology, London, UK

⁵ Department of Developmental Biology, Stanford University School of Medicine, Stanford, CA USA

⁶ Department of Structural Biology, Stanford University School of Medicine, Stanford, CA USA

⁷ UK Dementia Research Institute at UCL, UCL Institute of Neurology, London, UK.

⁸ Department of Genetics, Evolution and Environment, Institute of Healthy Ageing, University College London, London, UK

⁹ Department of Stem Cell Biology and Regenerative Medicine, Eli and Edythe Broad Center for Regenerative Medicine and Stem Cell Research, University of Southern California, Los Angeles, CA USA

¹⁰ Stanford Neurosciences Graduate Program, Stanford University School of Medicine, Stanford, CA, USA

Abstract

Nucleotide repeat expansions in the *C9orf72* gene are the most common cause of amyotrophic lateral sclerosis (ALS) and frontotemporal dementia (FTD). Unconventional translation (RAN

Users may view, print, copy, and download text and data-mine the content in such documents, for the purposes of academic research, subject always to the full Conditions of use:http://www.nature.com/authors/editorial_policies/license.html#terms

¹¹Correspondence to: agitler@stanford.edu.

Contributions

This work was performed and written by S.B.Y. under the mentorship of A.D.G. T.F.G. contributed ELISA assays to detect RAN peptides and analyses under the mentorship of L.P. T.N., I.G., and A.T. contributed *Drosophila* studies under the mentorship of L.P. and A.M.I. N.R.G. contributed to polysome profiling studies and analyses, under the mentorship of M.B. R.G. contributed to RAN translation studies and analyses, under the mentorship of J.D.P. Y.S. and G.R. contributed induced motor neuron studies and analyses, under the mentorship of J.K.I. N.J.K. contributed to studies of *ATXN2* RAN translation. L.N., S.F., and T.J.I.D. contributed to studies of *C9orf72* RAN translation.

Competing Interests

A.D.G. has served as a consultant for Aquinnah Pharmaceuticals, Prevail Therapeutics, and Third Rock Ventures

translation) of *C9orf72* repeats generates dipeptide repeat proteins that can cause neurodegeneration. We performed a genetic screen for regulators of RAN translation and identified small ribosomal protein subunit 25 (*RPS25*), presenting a potential therapeutic target for c9ALS/FTD and other neurodegenerative diseases caused by nucleotide repeat expansions.

The most common genetic cause of ALS and FTD is a mutation in the *C9orf72* gene^{1,2}. The mutation is an expansion of the repetitive nucleotide tract GGGGCC within the first intron of *C9orf72*. The expanded nucleotide repeat is translated by an unconventional form of translation, called repeat-associated non-AUG (RAN) translation to produce dipeptide repeat (DPR) proteins³⁻⁷. These DPRs are aggregation-prone, accumulate in the central nervous system of patients and could cause disease through a protein toxicity mechanism. Insight into the mechanism of RAN translation requires analysis of the sequence features promoting RAN translation⁸⁻¹⁰ and the identification of regulators.

We discovered that RAN translation occurs in yeast (Fig. 1a), indicating it exploits an evolutionarily conserved process or machinery and, importantly, providing the opportunity to discover genes required for this process. We designed a genetic screen to identify genes that specifically affected RAN translation but not repeat RNA levels or general translation (Fig. 1b). We assembled a library of 275 yeast mutants for genes encoding translational machinery, including ribosomal subunits and other translation factors (Supplementary Table S1). We introduced a galactose-inducible *C9orf72* 66 repeat construct into each strain by transformation and used a poly(GP) immunoassay to gauge levels of RAN translation. To identify hits that specifically affected RAN translation and not general translation, we counter-screened hits by assessing their effect on the expression of an ATG-initiated GFP construct. We identified 42 genes that either increased or decreased DPR levels without similarly regulating ATG-GFP (Fig. 1c and Fig. S1a-c). We also performed quantitative reverse transcription polymerase chain reaction (RT-qPCR) to identify hits that affected transcription or RNA stability of the repeat RNA (Supplementary Table S1).

One striking hit from our screen was the deletion of *RPS25A*. *RPS25A* encodes a eukaryotic-specific, non-essential protein component of the small (40S) ribosomal subunit^{11,12}. *RPS25* plays a critical role in several forms of unconventional translation including IRES-mediated translation and ribosomal shunting¹³. *RPS25* mediates the direct recruitment of the 40S ribosomal subunit to the Cricket Paralysis Virus IRES RNA. It also regulates translation initiation of hepatitis C virus and picornaviral IRES RNAs, downstream of 40S subunit recruitment¹¹⁻¹⁴. In addition to viral RNAs, *RPS25* regulates several cellular IRES containing RNAs including p53 and c-myc^{13,15}. Deleting *RPS25A* (*tps25A*) reduced levels of RAN translated poly(GP) by 50% compared to wildtype yeast (Fig. 1c,d). Deletion of *RPS25A* did not affect the levels of GFP or the abundance of GGGGCC repeat RNA (Fig. S1 d-f).

In mammals, there is a single *RPS25* homolog, ribosomal protein S25 (*RPS25*). To test if the function of *RPS25* in regulating RAN translation is conserved from yeast to human, we analyzed a human cell line (Hap1) harboring a CRISPR-induced knockout of *RPS25*¹². We transfected a 66 repeat construct analogous to the one we used for the yeast experiments into Hap1 *RPS25* knockout cells. *RPS25* knockout resulted in ~50% reduction poly(GP) levels

without affecting the levels of repeat RNA (Fig. 1e and Fig. S2a). Because RAN translation can occur in multiple reading frames of the GGGGCC repeat, we also tested effects of *RPS25* knockout on another reading frame and found the Glycine-Alanine (GA) frame was reduced by over 90% compared to WT (Fig. 1f,g). Finally, we found that *RPS25* knockout reduced Glycine-Arginine (GR) levels by ~30%, comparable to control cells not expressing the GGGGCC repeat (Fig. 1h, Fig. S2b). The higher level of background poly(GR) signal in this immunoassay, even after *RPS25* knockout, likely reflects the abundance of GR repeats in the proteome (e.g., RGG/RG motifs)¹⁶.

To test the impact of *RPS25* knockout on global translation, we performed puromycin-incorporation assays. Consistent with previous observations^{11,13}, *RPS25* knockout did not affect global translation (Fig. S2ce). Furthermore, *RPS25* knockout did not significantly alter cell growth rate or expression of a canonically translated ATG-Clover reporter (Fig. S2 f–j). *RPS25* knockout had only mild effects on polysome profiles, a global measure of actively translated mRNAs (Fig. S3 a,b). Notably, while nearly all profile peak to 40S ratios remained similar, the 60S/40S and heavy polysome/40S ratios were increased in *RPS25* knockout cells, providing evidence that global translation is not significantly impaired in *RPS25* knockout cells. RT-qPCR analysis from RNA associated with different fractions of the polysome profile, illustrated that there is no decrease in heavy polysome-associated (generally thought to be highly translated) *ACTB* or GFP (Fig. S3c,d). Importantly, there was less GGGGCC RNA associated with heavy polysomes in *RPS25* knockout cells compared to wildtype (Fig. S3e), consistent with decreased translation of GGGGCC RNA in *RPS25* knockout cells. These data are consistent with a role of RPS25 as a regulator of RAN translation of the *C9orf72* repeat expansion.

How generalizable is the effect of RPS25 knockout on RAN translation? Is RPS25 required for efficient RAN translation of other nucleotide repeat expansions? First, we generated *ATXN2* CAG repeat constructs, mutating all ATG codons upstream of the CAG repeats and placing a myc/his tag in frame with poly-Alanine (poly(A)) RAN products (Fig. S4a,b). We then generated a HeLa cell line with a CRISPR-induced mutation in *RPS25*, which markedly reduces levels of RPS25 (Fig. S4c–h). Consistent with other repeats, we only detect poly(A) and poly(Q) products in the longer *ATXN2* CAG repeat lengths (CAG58 and 108, Fig. 1i–k). Expression of both of these reading frames was reduced in the RPS25 mutant HeLa cell line (Fig. 1i–k and Fig. S4g–i). Next, we tested RAN translation of mutant huntingtin protein (Htt). RPS25 reduction in HeLa cells reduces poly(A) RAN products expressed from unmodified HTT CAG repeats but does not significantly reduce the expression of poly(Q) which initiates from the native ATG codon of *HTT* (Fig. S4j–l and Table S2). Thus, RPS25 is required for efficient RAN translation of both CAG and GGGGCC repeats.

To extend our findings to a more clinically relevant system, we next asked if RPS25 regulates RAN translation of *C9orf72* repeats expressed from their endogenous context and at physiological levels in cells obtained from humans with ALS. We analyzed cultured induced pluripotent stem cells (iPSCs) from two healthy subjects and three ALS patients with *C9orf72* repeat expansions. Reduction of RPS25 levels by siRNA significantly reduced the levels of poly(GP) compared to the non-targeting control (Fig. 2a,b, Fig. S5a,b, and

Table S3). Importantly, RPS25 reduction did not influence the number of RNA foci (Fig. 2c–e) or levels of the different *C9orf72* alternative transcript variants, including transcripts specifically harboring the GGGGCC repeat (Fig. 2f,g), indicating RPS25 functions at the level of translation without impacting repeat RNA transcription, stability, or foci formation. RPS25 reduction did not alter endogenous *C9orf72* protein expression (Fig. S5c). Thus, RPS25 regulates the endogenous RAN translation of *C9orf72* nucleotide repeat expansions in the poly(GP) frame.

We next tested if inhibiting RPS25 could mitigate neurodegenerative phenotypes caused by *C9orf72* repeat expansions *in vivo*. We used transgenic *Drosophila* engineered to express 36 GGGGCC repeats under the control of the inducible elav-GeneSwitch driver. Consistent with previous reports¹⁷, neuronal expression of 36 repeats resulted in the production of DPRs (Fig. 3a,b) and shortened lifespan (Fig. 3c). Reducing the expression of *Drosophila* Rps25 using RNAi lowered poly(GP) levels (Fig. 3a,b and Fig. S6) and significantly increased the lifespan of 36 repeat-expressing adult, male flies (Fig. 3c and Fig. S7a,e,g). Notably, as a control, we reduced Rps25 in flies engineered to express 36 Glycine-Arginine dipeptide codon-optimized repeats driven from an ATG (36GR) and not in the context of a repetitive GGGGCC tract¹⁷ and therefore do not undergo RAN translation. Reducing Rps25 levels did not rescue the shortened lifespan of 36GR flies (Fig. 3d), providing evidence that Rps25 functions upstream or at the level of production of the toxic DPRs. Rps25 RNAi did not affect the lifespan of WT male flies (Fig. 3c and Fig. S7f). Thus, Rps25 regulates RAN translation in the poly(GP) frame and the pathogenicity of *C9orf72* GGGGCC repeats in the nervous system of *Drosophila*.

Finally, to extend our studies to human neurons, we tested the impact of lowering *RPS25* levels on survival phenotypes in motor neurons from patients with ALS harboring endogenous *C9orf72* GGGGCC expansions. We used transcription factor mediated reprogramming to generate induced motor neurons (iMNs) from iPSCs from patients with *C9orf72* ALS and unaffected individuals, as previously described¹⁸. The c9ALS patient-derived iMNs showed reduced survival after glutamate addition compared to control iMNs (Fig. 3e and Fig. S8c,f,i). We tested two independent antisense oligonucleotides (ASOs) targeting *RPS25* and one non-targeting control ASO. Both *RPS25* ASOs significantly increased the proportion of surviving iMNs in the c9ALS line (Fig. 3e, Fig. S8c,f,i and Fig. S8a) but did not increase survival of control iMNs (Fig. S8b). Furthermore, both *RPS25* ASOs significantly reduced the number of poly(GR) and poly(PR) foci in c9 ALS patient-derived iMNs (Fig. 3f,g, Fig. S8d,e,g,h,j,k, Fig. S9, and Fig. S10).

Here, we found that RPS25 is selectively required for the efficient RAN translation of expanded GGGGCC repeat expansions in the *C9orf72* gene and CAG expansions in *ATXN2* and *HTT*. We present a novel RAN translation regulator as a potential therapeutic target and suggest that strategies to inhibit the function of RPS25 could be pursued as an effective therapy for c9ALS/FTD and perhaps other neurodegenerative diseases caused by nucleotide repeat expansions^{19,20}.

Online Methods

Yeast strains and plasmids

Yeast experiments were conducted using the wildtype haploid strain BY4741 (derived from S288C). For validation of screen results, deletions of *RPS25A* was generated using PCR and homologous recombination to replace each open reading frame (ORF) with a NatMX resistance cassette to generate the null allele, *yps25A* ::NatMX. Sense strand *C9orf72* hexanucleotide repeats with (GGGGCC)₂, (GGGGCC)₄₀, and (GGGGCC)₆₆ described previously were used for this study²¹. The 2-micron galactose promoter plasmid pAG426GAL was used for the ribosomal miniscreen and the centromeric galactose promoter plasmid pAG416GAL was used for validations²². Cross validation was performed using pAG426GAL GFP plasmids from the Addgene Yeast Gateway Kit (Kit #100000011)²². Plasmids were introduced into yeast strains using standard lithium acetate transformation for individual transformations. For the ribosomal miniscreen, a 96-well transformation was employed^{23,24}.

Yeast lysate preparation and immunoblotting

For the ribosome miniscreen, overnight yeast cultures grown in 2% raffinose-containing media were diluted into 2% galactose-containing media to induce transgene expression from a 426 GAL C940R plasmid, and were further grown for 12 hours with shaking at 30°C. For individual validations, yeast were prepared as above, driving expression from a 416 GAL C966R plasmid and grown in galactose for eight hours. Yeast cells were harvested by centrifugation (3000×g for 5 minutes), resuspended in lysis buffer [Y-Per™ Plus (ThermoFisher Scientific), 2X Halt Protease Inhibitor Cocktail (ThermoFisher Scientific)], and incubated for 20 minutes at room temperature. Lysates were clarified by centrifugation (10,000×g at 4°C for 10 minutes) and soluble lysates were subjected to immunoassays.

Yeast protein lysates were quantified using bicinchoninic acid (Pierce BCA) assays and 20µg of protein was loaded with 1X NuPAGE LDS sample buffer, and 50mM dithiothreitol, and denatured for 10 minutes at 70°C. Samples were loaded onto 4–12% Bis-Tris gels and subjected to PAGE. Gels were transferred to 0.45µm nitrocellulose membranes (Bio-Rad) using semi-dry transfer (Bio-Rad Trans-Blot SD Semi-Dry Cell) and 2X, 10% methanol NuPAGE transfer buffer (Novex) at 17V for one hour. Membranes were blocked in Odyssey Blocking Buffer and probed with rabbit anti-GFP (1:1000, ThermoFisher Scientific A-11122) and mouse anti-GAPDH (1:5000, Sigma G8795) and HRP-conjugated secondary antibodies.

Yeast RT-qPCR

For the yeast miniscreen, yeast were grown as described above. Yeast were harvested in TRIzol (ThermoFisher Scientific) and RNA was extracted using a combination of chloroform and the RNA Clean & Concentrator ZR-96 kit (Zymo Research) according to manufacturer's protocol. 5µL of RNA was loaded for the RT reaction using the High Capacity cDNA kit (Applied Biosystems) and 1µL of a 1:10 cDNA dilution was utilized for 10µL qPCR reactions as described below.

RNA was extracted from yeast using a MasterPure Yeast RNA Extraction kit (Epicentre), including DNaseI digestions. 250ng of RNA were reverse transcribed into cDNA using High Capacity cDNA Reverse Transcription Kit with random primers (Applied Biosystems). cDNA products were diluted 1:10 and 2 μ L were analyzed by qPCR using custom primer sets and SYBR green reagent (20 μ L total reaction, PCR Master mix, Applied Biosystems). Primers used: scACT1 Fwd = 5' ATTCTGAGGTTGCTGCTTTGG; scACT1 Rev = 5' TGTCTTGGTCTACCGACGATAG; C9repeat Fwd = 5' AGCTTAGTACTCGCTGAGGGTG; C9repeat Rev = 5' GACTCCTGAGTTCCAGAGCTTG. The $2^{-\Delta\Delta Ct}$ method was used to determine the relative mRNA expression of each gene.

Poly(GP) enzyme-linked immunosorbent assay (ELISA)

Poly(GP) levels in lysates were measured in a blinded fashion using a previously described sandwich immunoassay that utilizes Meso Scale Discovery electrochemiluminescence detection technology, and an affinity purified rabbit polyclonal poly(GP) antibody (Rb9259) as both capture and detection antibody²⁵⁻²⁸. Lysates were diluted to the same concentration using Tris-buffered saline (TBS) and tested in duplicate wells. Response values corresponding to the intensity of emitted light upon electrochemical stimulation of the assay plate using the Meso Scale Discovery QUICKPLEX SQ120 were acquired. All responses were background corrected using the response from the negative control samples. In some cases when comparing across mutants or iPSC lines, poly(GP) responses were then normalized to our positive control.

Poly(GR) enzyme-linked immunosorbent assay (ELISA)

GR MSD immunoassays were performed as previously described using an affinity purified rabbit polyclonal anti-GR antibody²⁹ with the following modification: cells were lysed in RIPA buffer containing 0.5 M urea and 2X protease inhibitors (Roche cComplete mini EDTA-free) and 180 μ g protein loaded per well.

Yeast anti-GFP enzyme-linked immunosorbent assay (ELISA)

The yeast ribosomal mutants were counter-screened for effect on levels of eGFP in the context of a Kozak sequence and ATG-initiation as a readout of general effects on translation. Yeast cells were induced with galactose and lysed as previously described. Lysates were diluted 1:50 to fit in the range of detection and the manufacturer's protocol was followed without changes (Abcam, ab175181). Signal from mutants expressing eGFP divided by total μ g of protein loaded for the ELISA was normalized as a ratio of wildtype eGFP expression and compared to effect of mutants on poly(GP) expression.

Mammalian cell culture and treatments

Hap1 wildtype and RPS25 knockout cell lines¹² were cultured in standard conditions using IMDM (ThermoFisher Scientific) with 10% FBS and penicillin-streptomycin. HeLa cell lines were cultured similarly in DMEM (ThermoFisher Scientific). For *C9orf72* GGGGCC transfections, we used mammalian expression vectors under CAG promoter, empty cassette or GGGGCC₂ or GGGGCC₆₆ (C9 2R and C9 66R) and with 3 epitope tags/frame.

Transfections of these plasmids were performed with Lipofectamine 3000 (ThermoFisher Scientific) using the manufacturer's protocol. After 12 hour transfection, media was replaced with fresh IMDM. Hygromycin (300µg/µL, Invivogen) was added at 24 hours for selection and cells were harvested 72 hours after transfection.

ATXN2 RAN construct generation

Variable length CAG repeats (22, 31, 39, 58, 108 repeat-length) were cloned from human *ATXN2* cDNA and subsequently sub-cloned into a pCDNA6-myc-His-A expression vector using standard molecular cloning techniques (the C' myc-6xHis epitope tags in frame with the poly-A encoding forward reading frame). 38 bp upstream and 98 bp downstream of the CAG repeats in the human *ATXN2* gene were included in the construct. All ATG codons upstream of the CAG repeat region identified in any forward reading frame were mutated from ATG to AAG using site directed mutagenesis (Agilent, QuikChange II Site-Directed Mutagenesis Kit), or the mutations were introduced with primers during PCR. Constructs were verified by sanger sequencing before transfection.

HeLa RPS25KD mutant generation

HeLa cells constitutively expressing Cas9-BFP were kindly gifted by Dr. Michael Bassik. Two RPS25 guides were cloned and lentivirus was generated as described previously²⁷. HeLa-Cas9 cells were subsequently treated with zeocin in order to select for RPS25-guide infected cells. Cells were subsequently subcloned and screened via immunoblotting to find the RPS25KD clone used in this study. RPS25 guide sequence provided by the Bassik laboratory: CACCGTGGTCCAAAGGCAAAGTTC. RPS25 guide sequence generated using Benchling software: CACCGCTTCTTTTTGGCCTTGCCCC. HeLa control cells used in our experiments were derived from the same original HeLa Cas9-BFP population and infected with guides containing a safe, non-gene-targeting sequence provided by the Bassik laboratory. Safe guide sequence: GTCCCCCTCAGCCGTATT.

Mammalian cell RT-qPCR

24-well plates of Hap1 or HeLa wildtype or mutant cell lines were harvested using the PureLink RNA Mini Kit (Life Technologies) using manufacturer's protocol. 250–500ng of RNA was used for reverse transcription into cDNA using the High Capacity cDNA Reverse Transcription Kit (ThermoFisher Scientific). cDNA was subsequently diluted 1:10 and 2µL was analyzed using qPCR with custom primer sets and SYBR green reagent (PCR Master mix, Applied Biosystems). Primers used: C9repeat Fwd = 5'AGCTTAGTACTCGCTGAGGGTG; C9repeat Rev = 5'GACTCCTGAGTTCCAGAGCTTG. hActin (ActB) Fwd= ATTCTGAGGTTGCTGCTTTGG, hActin (ActB) Rev= TGTCTTGGTCTACCGACGATAG. ATXN2 construct Fwd= TCCTCTCTAGAGGGCCCTTC, ATXN2 construct Rev= TCAATGGTGATGGTGATG. HTT construct Fwd= GCAGGCACAGCCGCTGCTGC, HTT construct Rev= GGTGGTGCAGCGGCTCCTC. 18S Fwd = AGAAACGGCTACCACATCCA, 18S Rev= CACCAGACTTGCCCTCCA. rLuc Fwd= TGGAGAATAACTTCTTCGTGGA, rLuc Rev= TTGGACGACGA ACTTCAACC. The 2exp (- Ct) method was used to determine the relative mRNA expression of each gene.

Mammalian cell lysate preparation and immunoblotting

Hap1 or HeLa cells were transfected and treated as above prior to lysis. Cells were washed twice in ice-cold 1X PBS and lysed in ice-cold RIPA buffer supplemented with 1X HALT Protease Inhibitor cocktail (Pierce). Lysate was clarified at 10,000×g for 10 minutes at 4°C, and protein concentration was measured using bicinchoninic acid (Pierce BCA) assays. 20–25µg of protein were prepared in 1X SDS buffer and 2.5% beta mercaptoethanol (Sigma) and denatured for 5 minutes at 95°C. Samples were loaded and resolved as previously described. Transfer was conducted as previously described using 0.45µm PVDF activated briefly in 100% methanol (for poly(GA) analysis) and 0.45µm nitrocellulose for all other immunoblotting. Odyssey blocking buffer was used to block and for antibody solutions, with the exception of anti-His solutions that were made using 5% BSA in TBST. Antibodies were as follows: rabbit anti-HA (1:1000, Cell Signaling 3724), mouse anti-GAPDH (1:5000, Sigma G8795), rabbit anti-RPS25 (Abcam ab102940), mouse anti-HIS (1:1000, EMD Millipore05–949), mouse anti-polyGlutamine (1:1000, EMD Millipore 5TF1–1C2), rabbit anti-C9orf72 (1:1000, sc-138763), rabbit poly(GP) (1:1000, EMD Millipore ABN1358) and rabbit anti-poly(A) c-terminal-specific RAN antibody (1:2000, generously shared by the Ranum laboratory)³⁰.

For puromycin incorporation assay, 0.45µm nitrocellulose was used and antibodies include: mouse anti-puromycin (1:1000, EMD Millipore MABE343) and mouse anti-GAPDH were probed on separate replicate blots. Secondary antibodies include: goat anti-mouse HRP (1:5000, Fisher 62–6520), goat anti-rabbit HRP (1:5000, Fisher 31462), goat anti-mouse Alexa Fluor 790 (1:20,000, Fisher A11371), and goat anti-rabbit Alexa Fluor 680 (1:20,000, Fisher A21109).

Hap1 puromycin-incorporation assay

Hap1 wildtype and RPS25 knockout cells were treated with 10µg/mL of puromycin for 10 minutes prior to lysis and immunoblotting.

Hap1 Clover (GFP variant) expression via flow cytometry

pcDNA3.1 CMV-ATG-Clover constructs were transfected into Hap1 wildtype and RPS25 knockout cells with Lipofectamine 3000. After 48 hours of transient transfection, Hap1 cells were dissociated and resuspended in 1X PBS, 2% FBS, 1mM EDTA buffer and analyzed in the FITC channel for GFP expression using a Guava easyCyte Single Sample Flow Cytometer (EMD Millipore). Data was analyzed using Flowjo (version X 10.0.7r2) and the mean GFP signal was calculated.

Hap1 growth curve analysis

Hap1 wildtype and RPS25 knockout cells were seeded at 1.5×10^5 cells into a 12-well plate and imaged with a 10X objective every 4 hours using the InCuCyte (Essen BioScience). Phase-contrast images were analyzed using the InCuCyte default analysis software to compute percent confluency. Technical replicate average was determined over 9 images collected throughout each well at each time point to account for differences in growth depending on image point within plates. Biological average across independent wells is

plotted in Fig. S2. Area under the curve calculations and statistics were performed using the GraphPad Prism analysis option for Area under the curve.

Ribosome fractionation and RT-qPCR

Hap1 wildtype and RPS25 knockout cells transfected with C9 66R plasmid were lysed in lysis buffer (20mM Tris pH 7.5, 150mM NaCl, 15mM MgCl₂, 100µg/ml cycloheximide (Sigma), 1mM dithiothreitol, 0.5% Triton X-100, 0.1mg/ml heparin (Sigma), 8% glycerol, 20U/ml TURBO™ DNase and 200U/mL SUPERase•In™ RNase Inhibitor (Invitrogen), 1X Halt Protease and Phosphatase Inhibitor Cocktail (ThermoFisher Scientific) and incubated for 30 min at 4°C. Lysates were clarified by sequential 1000×g and 10,000×g spins, taking the supernatant each time. 200µL of lysate was loaded onto a 10–45% sucrose gradient (20mM Tris pH 7.5, 100mM NaCl, 15mM MgCl₂, 100µg/ml cycloheximide, sucrose) and centrifuged for 2.5 hours at 40,000rpm in an SW40 rotor at 4°C. Gradients were fractionated on a Brandel Gradient fractionator at 30 second fraction intervals. Renilla luciferase RNA spike-in was added at 50pmol/fraction and used as a normalization control. RNA from each fraction was isolated with phenol-chloroform and precipitated using standard isopropanol extraction. 500ng is loaded into each RT reaction, fractions were pooled and included free RNPs, 40S, 60S, 80S, 2 polysomes, and selected fractions from heavy polysomes (as indicated in Fig. S3).

Human induced pluripotent stem cell (iPSC) culture and treatments

Ichida lab lymphocytes from healthy subjects and ALS patients were obtained from the NINDS Biorepository at the Coriell Institute for Medical Research and reprogrammed into iPSCs as described previously¹⁸. Target ALS patient iPSCs were obtained through the NINDS Human Cell and Data Repository. The NINDS Biorepository requires informed consent from patients. Rothstein lab iPSCs were collected from patients at Johns Hopkins Hospital with patient's consent and deidentification. Control iPSCs derived from fibroblasts from Pasca lab were collected from patients under informed consent with approval from the Stanford Human Stem Cell Research Oversight (SRCO) committee. Information on patient-derived iPSCs can be found in Table S3.

Matrigel was prepared according to manufacturer's protocol in DMEM/F12, coated on plates and incubated for 1 hour. Human control and patient-derived iPSCs were maintained on Matrigel (Corning) coated plates using mTeSR1 (STEMCELL Technologies) medium changed every day. iPSCs were dissociated with Accutase (STEMCELL Technologies) in the presence of ROCK inhibitor Y-27632 (Sigma) at 10µM overnight.

For siRNA transfections, first siRNA-lipofectamine complexes were prepared. Non-targeting and RPS25-targeting siRNAs (Dharmacon, Smartpool ON-TARGETplus Smartpool: D-001810–10-05 and L-013629–00-0005, respectively) are prepared in the following ratios: for a 24-well plate, 13µL of OptiMEM (ThermoFisher Scientific) with 1.25µL Lipofectamine RNAiMAX (ThermoFisher Scientific). Separately, 13µL of OptiMEM is mixed with 9pmol of siRNA and mixed with RNAiMAX mixture and incubated for 15 minutes. iPSCs were dissociated as previously and resuspended in 26µL of the siRNA-RNAiMAX mixture prepared above and incubated at room temperature for 10 minutes

(maximum time is 15 minutes). Cells and siRNA mixture were then added to Matrigel pre-coated wells with 0.5mL mTeSR plus Y-27632. Cells are maintained in Y-27632 for 12 hours until media was exchanged for fresh mTeSR. Cells were harvested 72 hours post-transfection.

Human iPSC RNA Fluorescence in situ hybridization (FISH) and quantification

RNA FISH was performed as previously reported²¹. iPSCs treated with RNAi as above were grown on Matrigel-coated coverslips, fixed in 4% paraformaldehyde and permeabilized with 0.2% Triton/DEPC-PBS. Slides were dehydrated with a series of ethanol washes and incubated with hybridization solution. LNA probes to detect sense (/5TYE563/CCCCGGCCCGGCC) or antisense (/5TYE563/GGGGCCGGGGCCGGGG) C9orf72 repeats were prepared and diluted to 100nM. After hybridization, the cells were incubated with the diluted LNA probes at 66°C for 24 h. Cells were then washed and counterstained with Hoechst 33258 (1µg/ml, Thermo Fisher Scientific). Afterward, the cells were dehydrated with ethanol washes and coverslips were mounted using ProLong Diamond antifade mountant. Images were obtained on a Leica DM16000B inverted fluorescence microscope with a 60X oil immersion objective. To quantify foci, 3 coverslips per treatment were analyzed and >200 nuclei were counted per coverslip. Counts were used to determine average number of foci per Hoescht positive nuclei since iPSCs grow in dense colonies where it is difficult to distinguish which cytoplasm a particular focus resides in.

Foci were quantified in an unbiased manner using the MetaXpress granularity software which detects foci of a determined size range compared to changes in surrounding pixel intensity. Parameters used for this analysis were 2–7px in diameter and pixel intensity change of 3500 grey levels. Hoechst-positive nuclei were counted using the Analyze Particle function in Fiji. In brief, all images across treatments were stacked, converted to 8-bit and thresholded to the same value prior to the Analyze Particle function in order to ensure that every image was quantified uniformly across conditions and coverslips.

Human iPSC and iMN RT-qPCR analysis

Human iPSCs were treated with siRNAs, RNA extraction and RT were set-up as described above. Human iPSC-derived iMNs were treated with ASOs for 72 hours prior to freezing in TRIzol (ThermoFisher Scientific), then RNA was extracted using standard TRIzol-chloroform extraction protocols. Reverse transcriptions reactions were setup as described above. Custom Taqman probes for C9orf72 and standard Taqman probes for hActin (ThermoFisher Scientific, Hs01060665_g1) and RPS25 (ThermoFisher Scientific, Hs01568661_g1) were used with the TaqMan Universal Master Mix II (Applied Biosystems, 440040). Custom probes were as follows: C9 total isoforms FWD: TGTGACAGTTGGAATGCAGTGA, C9 total isoforms REV: GCCACTTAAAGCAATCTCTGTCTTG, C9 expansion isoforms FWD: GGGTCTAGCAAGAGCAGGTG, C9 expansion isoforms REV: GTCTTGGCAACAGCTGGAGAT.

Drosophila husbandry

All flies were reared at 25°C on a 12-hr:12-hr light:dark (LD) cycle at constant humidity and on standard sugar-yeast-agar (SYA) medium (agar, 15 g/l; sugar, 50 g/l; autolyzed yeast, 100 g/l; nipagin, 100 g/l; and propionic acid, 2 ml/l).

Drosophila lifespan analysis

Flies were raised at standard density in 200ml bottles. After eclosion, flies were allowed to mate for 24–48 hours. Females or males of the appropriate genotype were split into groups of 15 and housed in vials containing SYA medium with or without 200µM RU486 to induce the gene-switch driver. Deaths were scored and flies tipped onto fresh food 3 times a week. Data are presented as cumulative survival curves, and survival rates were compared using log-rank tests. All lifespans were performed at 25°C. ElavGS was derived from the original elavGS 301.2 line³¹ and obtained as a generous gift from Dr. H. Tricoire (CNRS). UAS-36(GGGGCC) and UAS-36GR lines have previously described¹⁷, UAS-RpS25 RNAi lines P{GD10582}v52602 and P{KK107958}VIE-260B were obtained from Bloomington stock center.

Drosophila immunoblotting

Protein samples were prepared by homogenizing in 2x SDS Laemmli sample (4% SDS, 20% glycerol, 120 mM Tris-HCl (pH 6.8), 200 mM DTT with bromophenol blue) and boiled at 95°C for 5 min. Samples were separated on pre-cast 4%–12% Invitrogen Bis-Tris gels (NP0322), blotted onto PVDF membrane, blocked in 5% milk in TBST and incubated with anti-GP polyclonal rabbit antibody (1:1000)¹⁷, or mouse anti-actin (Abcam ab8224) (1:10000) followed by horseradish peroxidase-tagged secondary antibody (anti-rabbit HRP, ab6721 or anti-mouse HRP, ab6789, Abcam, 1:10,000). The protein standard used as a molecular weight ladder was MagicMark™ XP Western Protein Standard (Thermoscientific, LC5602)

Drosophila RT-qPCR

Total RNA was extracted from 8 flies per sample using TRIzol (GIBCO) according to the manufacturer's instructions. The concentration of total RNA purified for each sample was measured using an Eppendorf biophotometer. One microgram of total RNA was then subjected to DNA digestion using DNase I (Ambion), immediately followed by reverse transcription using the SuperScript® II system (Invitrogen) with oligo(dT) primers. Quantitative PCR was performed using the PRISM 7000 sequence-detection system (Applied Biosystems), SYBR® Green (Molecular Probes), ROX Reference Dye (Invitrogen), and HotStarTaq (Qiagen) by following the manufacturer's instructions. Each sample was analysed in duplicate and values are the mean of four independent biological repeats ± SEM. Primers used were: RpS25 Fwd: AAATCGAACAGCTGACGTGC, RpS25 Rev: AAAATACATTTTCAGCGGCTG.

Conversion of iPSCs into induced motor neurons

Reprogramming was performed in 96-well plates (8×10^3 cells/well) or 13mm plastic coverslips (3.2×10^4 cells/coverslip) that were sequentially coated with gelatin (0.1%, 1

hour) and laminin (2–4 hours) at room temperature. To enable efficient expression of the transgenic reprogramming factors, iPSCs were cultured in fibroblast medium (DMEM + 10% FBS) for at least 48 hours and either used directly for retroviral transduction or passaged before transduction for each experiment. Retroviruses encoding the 7 iMN factors (*Ngn2*, *Isl1*, *Lhx3*, *Neurod1*, *Ascl1*, *Brn2*, *Myt1l*) in a pMXs backbone were added in 100–200 μ l fibroblast medium per 96-well well with 5 μ g/ml polybrene. For iMNs, cultures were transduced with lentivirus encoding the *Hb9::RFP* reporter 48 hours after transduction with transcription factor-encoding retroviruses. On day 5, primary mouse cortical glial cells from P1 ICR pups (male and female) were added to the transduced cultures in glia medium containing MEM (Life Technologies), 10% donor equine serum (HyClone), 20% glucose (Sigma-Aldrich), and 1% penicillin/streptomycin. On day 6, cultures were switched to N3 medium containing DMEM/F12 (Life Technologies), 2% FBS, 1% penicillin/streptomycin, N2 and B27 supplements (Life Technologies), 7.5 μ M RepSox (Selleck), and 10 ng/ml each of GDNF, BDNF, and CNTF (R&D). The iMN and iDA neuron cultures were maintained in N3 medium, changed every other day, unless otherwise noted^{15,27,32}.

Lentivirus production

All shRNA and *Hb9::RFP*-encoding lentiviruses were produced as follows: HEK293T cells were transfected at 80–90% confluency with viral vectors containing the genes of interest and viral packaging plasmids (pPAX2 and VSVG for lentivirus) using polyethylenimine (PEI)(Sigma-Aldrich). The medium was changed 24h after transfection. Viruses were harvested at 48 and 72 hours after transfection. Viral supernatants were filtered with 0.45 μ m filters and concentrated by incubating with Lenti-X concentrator (Clontech) for 24 hours at 4°C and centrifuging at 1,500 \times g at 4°C for 45 minutes. The pellets were resuspended in 300 μ l DMEM + 10% FBS and stored at –80°C.

7F iMN survival assay

On day 3 of iMN conversion, the cultures were incubated with scrambled or RPS25-targetting ASOs (9 μ M) with 5 μ g/ml polybrene in N3 media containing DMEM/F12 (Life Technologies), 2% FBS, 1% penicillin/streptomycin, N2 and B27 supplements (Life Technologies), and 10 ng/ml each of GDNF, BDNF, and CNTF (R&D). All shRNA constructs were tagged with GFP to enable specific tracking of Dox-NIL iMNs expressing the shRNAs. On day 5, primary mouse cortical glial cells from P1 ICR pups (male and female) were added to the transduced cultures in N3 media containing 7.5 μ M RepSox (Selleck). *Hb9::RFP*⁺ iMNs appeared between days 13–16 after retroviral transduction. RepSox was removed at day 17 and the survival assay was initiated by adding 10 μ M glutamate to the culture medium for 12 hours. Cells were then maintained in N3 medium with neurotrophic factors without RepSox. Longitudinal tracking was performed by imaging neuronal cultures in a Molecular Devices ImageExpress once every 48 hours starting at day 17. Tracking of neuronal survival was performed using SVcell 3.0 (DRVision Technologies). Neurons were scored as dead when their soma was no longer detectable by RFP fluorescence. Neuron survival assays were performed in triplicate. To increase clarity, similar numbers of randomly selected neurons from each trial were combined to generate the quantification shown. ASO sequences as follows: RPS25–549 (ASO#2):
mG*mA*mG*mU*mC*T*C*A*T*T*C*T*G*T*T*mG*mC*mC*mC*mA, and RPS25–

2349 (ASO#1):

mG*mU*mU*mG*mC*A*T*T*C*C*G*C*T*G*mC*mC*mU*mC (with phosphothiorate bonds indicated by * and 2'O methylation indicated by m (gapmer design from IDT).

DPR immunocytochemistry

Control and patient-derived iMNs were treated with ASOs for 72 hours and subsequently fixed in 4% paraformaldehyde (PFA) for 1 hour at 4°C, permeabilized with 0.1% Triton-X/PBS 20 minutes at room temperature, blocked with 10% donkey serum in 3% BSA/PBS at room temperature for 2 hours, and incubated with primary antibodies with 0.3% BSA/PBS at 4 °C overnight. Cells were then washed with 0.1% PBS-T and incubated with Alexa Fluor® secondary antibodies (Life Technologies) in 0.3% BSA/PBS for 2 hours at room temperature. To visualize nuclei, cells were stained with DAPI (Life Technologies) or Hoechst and then mounted on slides with Vectashield® (Vector Labs). Images were acquired on an LSM 800 confocal microscope (Zeiss). The following primary antibodies were used: rabbit anti-poly(PR) (Proteintech 23979–1-AP, 1:50), rabbit anti-poly(GR) (Proteintech 23978– 1-AP, 1:50). 20 iMNs were quantified per genotype per condition. For quantifications of poly(GR) and poly(PR) nuclear puncta, the number of nuclear puncta were counted and divided by total nuclear area as outlined in Fig. S10.

Statistics

Statistical analyses were performed using GraphPad Prism7 and Microsoft Excel. Statistical tests included two-tailed t-test, one or two-way ANOVA and two-sided log-rank test for survival data. No power analyses were conducted in order to predetermine sample size, but our sample sizes are consistent those reported in previous publications^{15,17,18,21}. Data distribution was assumed to be normal, but this was not formally tested. No data or animals were excluded from analysis.

Randomization

Unless otherwise stated below, samples were not randomized or blinded during experiments or analysis.

For all poly(GP) and poly(GR) ELISAs, researchers were blinded to samples while performing and analyzing ELISA data. Researchers responsible for transfecting and lysing cells were not blinded.

For iPSC foci image quantifications, RNA foci and nuclei were quantified in an automated manner as described in the methods with no data being removed and did not require blinding.

For neuron survival assays, >50 neurons were selected for tracking randomly at day 1 of the assay. To select 50 iMNs per condition for analysis, the survival values for 50 cells were selected at random using the RAND function in Microsoft Excel. For other phenotypes, neurons were selected randomly for analysis. IMN survival times were confirmed by manual longitudinal tracking by an individual who was blinded to the identity of the genotype and

condition of each sample. All other quantification was performed by individuals blinded to the identity of each sample.

Data Availability

The data supporting the findings of this study are available from the corresponding author upon request.

Supplementary Material

Refer to Web version on PubMed Central for supplementary material.

Acknowledgments

This work was supported by NIH grants R35NS097263 (A.D.G.), AI099506 (J.D.P.), AG064690 (A.D.G. and J.D.P.), R35NS097273 (L.P.), P01NS099114 (T.F.G., L.P.), and R01NS097850 (J.K.I.), the Robert Packard Center for ALS Research at Johns Hopkins (L.P., A.D.G.), Target ALS (L.P., A.D.G., T.F.G.), the U.S. Department of Defense (J.D.P., A.D.G., J.K.I.), the Muscular Dystrophy Association (J.K.I.), 2T32HG000044–21 NIHGRI training grant (S.B.Y.), the Brain Rejuvenation Project of the Stanford Neurosciences Institute (A.D.G.), the European Research Council grant ERC-2014-CoG-648716 (A.M.I.), Alzheimer's Research UK (A.M.I.), and the MRC (A.M.I.). J.K.I. is a New York Stem Cell Foundation-Robertson Investigator. We thank Dr. Laura Ranum (University of Florida) for sharing the huntingtin poly-alanine antibody. We thank Dr. Michael Bassik for the HeLa Cas9-BFP cell lines.

References

1. Renton AE et al. A hexanucleotide repeat expansion in C9ORF72 is the cause of chromosome 9p21-linked ALS-FTD. *Neuron* 72, 257–68 (2011). [PubMed: 21944779]
2. DeJesus-Hernandez M et al. Expanded GGGGCC hexanucleotide repeat in noncoding region of C9ORF72 causes chromosome 9p-linked FTD and ALS. *Neuron* 72, 245–56 (2011). [PubMed: 21944778]
3. Mori K et al. The C9orf72 GGGGCC repeat is translated into aggregating dipeptide-repeat proteins in FTL/ALS. *Science* 339, 1335–8 (2013). [PubMed: 23393093]
4. Ash PE et al. Unconventional translation of C9ORF72 GGGGCC expansion generates insoluble polypeptides specific to c9FTD/ALS. *Neuron* 77, 639–46 (2013). [PubMed: 23415312]
5. Zu T et al. RAN proteins and RNA foci from antisense transcripts in C9ORF72 ALS and frontotemporal dementia. *Proc Natl Acad Sci U S A* 110, E4968–77 (2013). [PubMed: 24248382]
6. Gendron TF et al. Antisense transcripts of the expanded C9ORF72 hexanucleotide repeat form nuclear RNA foci and undergo repeat-associated non-ATG translation in c9FTD/ALS. *Acta Neuropathol* 126, 829–44 (2013). [PubMed: 24129584]
7. Gao FB, Richter JD & Cleveland DW Rethinking Unconventional Translation in Neurodegeneration. *Cell* 171, 994–1000 (2017). [PubMed: 29149615]
8. Cheng W et al. C9ORF72 GGGGCC repeat-associated non-AUG translation is upregulated by stress through eIF2alpha phosphorylation. *Nat Commun* 9, 51 (2018). [PubMed: 29302060]
9. Green KM et al. RAN translation at C9orf72-associated repeat expansions is selectively enhanced by the integrated stress response. *Nat Commun* 8, 2005 (2017). [PubMed: 29222490]
10. Tabet R et al. CUG initiation and frameshifting enable production of dipeptide repeat proteins from ALS/FTD C9ORF72 transcripts. *Nat Commun* 9, 152 (2018). [PubMed: 29323119]
11. Landry DM, Hertz MI & Thompson SR RPS25 is essential for translation initiation by the Dicistroviridae and hepatitis C viral IRESs. *Genes Dev* 23, 2753–64 (2009). [PubMed: 19952110]
12. Fuchs G et al. Kinetic pathway of 40S ribosomal subunit recruitment to hepatitis C virus internal ribosome entry site. *Proc Natl Acad Sci U S A* 112, 319–25 (2015). [PubMed: 25516984]

13. Hertz MI, Landry DM, Willis AE, Luo G & Thompson SR Ribosomal protein S25 dependency reveals a common mechanism for diverse internal ribosome entry sites and ribosome shunting. *Mol Cell Biol* 33, 1016–26 (2013). [PubMed: 23275440]
14. Nishiyama T, Yamamoto H, Uchiumi T & Nakashima N Eukaryotic ribosomal protein RPS25 interacts with the conserved loop region in a dicistroviral intergenic internal ribosome entry site. *Nucleic Acids Res* 35, 1514–21 (2007). [PubMed: 17287295]
15. Shi Y et al. Therapeutic potential of targeting IRES-dependent c-myc translation in multiple myeloma cells during ER stress. *Oncogene* 35, 1015–24 (2016). [PubMed: 25961916]
16. Thandapani P, O'Connor TR, Bailey TL & Richard S Defining the RGG/RG motif. *Mol Cell* 50, 613–23 (2013). [PubMed: 23746349]
17. Mizielinska S et al. C9orf72 repeat expansions cause neurodegeneration in *Drosophila* through arginine-rich proteins. *Science* 345, 1192–4 (2014). [PubMed: 25103406]
18. Shi Y et al. Haploinsufficiency leads to neurodegeneration in C9ORF72 ALS/FTD human induced motor neurons. *Nat Med* 24, 313–325 (2018). [PubMed: 29400714]
19. Cleary JD & Ranum LP New developments in RAN translation: insights from multiple diseases. *Curr Opin Genet Dev* 44, 125–134 (2017). [PubMed: 28365506]
20. Green KM, Linsalata AE & Todd PK RAN translation-What makes it run? *Brain Res* 1647, 30–42 (2016). [PubMed: 27060770]
21. Kramer NJ et al. Spt4 selectively regulates the expression of C9orf72 sense and antisense mutant transcripts. *Science* 353, 708–12 (2016). [PubMed: 27516603]
22. Alberti S, Gitler AD & Lindquist S A suite of Gateway cloning vectors for high-throughput genetic analysis in *Saccharomyces cerevisiae*. *Yeast* 24, 913–9 (2007). [PubMed: 17583893]
23. Cooper AA et al. Alpha-synuclein blocks ER-Golgi traffic and Rab1 rescues neuron loss in Parkinson's models. *Science* 313, 324–8 (2006). [PubMed: 16794039]
24. Gietz RD & Schiestl RH Large-scale high-efficiency yeast transformation using the LiAc/SS carrier DNA/PEG method. *Nat Protoc* 2, 38–41 (2007). [PubMed: 17401336]
25. Gendron TF et al. Poly(GP) proteins are a useful pharmacodynamic marker for C9ORF72-associated amyotrophic lateral sclerosis. *Sci Transl Med* 9(2017).
26. Gendron TF et al. Cerebellar c9RAN proteins associate with clinical and neuropathological characteristics of C9ORF72 repeat expansion carriers. *Acta Neuropathol* 130, 559–73 (2015). [PubMed: 26350237]
27. Kramer NJ et al. CRISPR-Cas9 screens in human cells and primary neurons identify modifiers of C9ORF72 dipeptide-repeat-protein toxicity. *Nat Genet* 50, 603–612 (2018). [PubMed: 29507424]
28. Su Z et al. Discovery of a biomarker and lead small molecules to target r(GGGGCC)-associated defects in c9FTD/ALS. *Neuron* 83, 1043–50 (2014). [PubMed: 25132468]
29. Simone R et al. G-quadruplex-binding small molecules ameliorate C9orf72 FTD/ALS pathology in vitro and in vivo. *EMBO Mol. Med* 10, 22–31 (2017).
30. Banez-Coronel M et al. RAN Translation in Huntington Disease. *Neuron* 88, 667–77 (2015). [PubMed: 26590344]
31. Osterwalder T, Yoon KS, White BH & Keshishian H A conditional tissue-specific transgene expression system using inducible GAL4. *Proc Natl Acad Sci U S A* 98, 12596–601 (2001). [PubMed: 11675495]
32. Son EY et al. Conversion of mouse and human fibroblasts into functional spinal motor neurons. *Cell Stem Cell* 9, 205–18 (2011). [PubMed: 21852222]

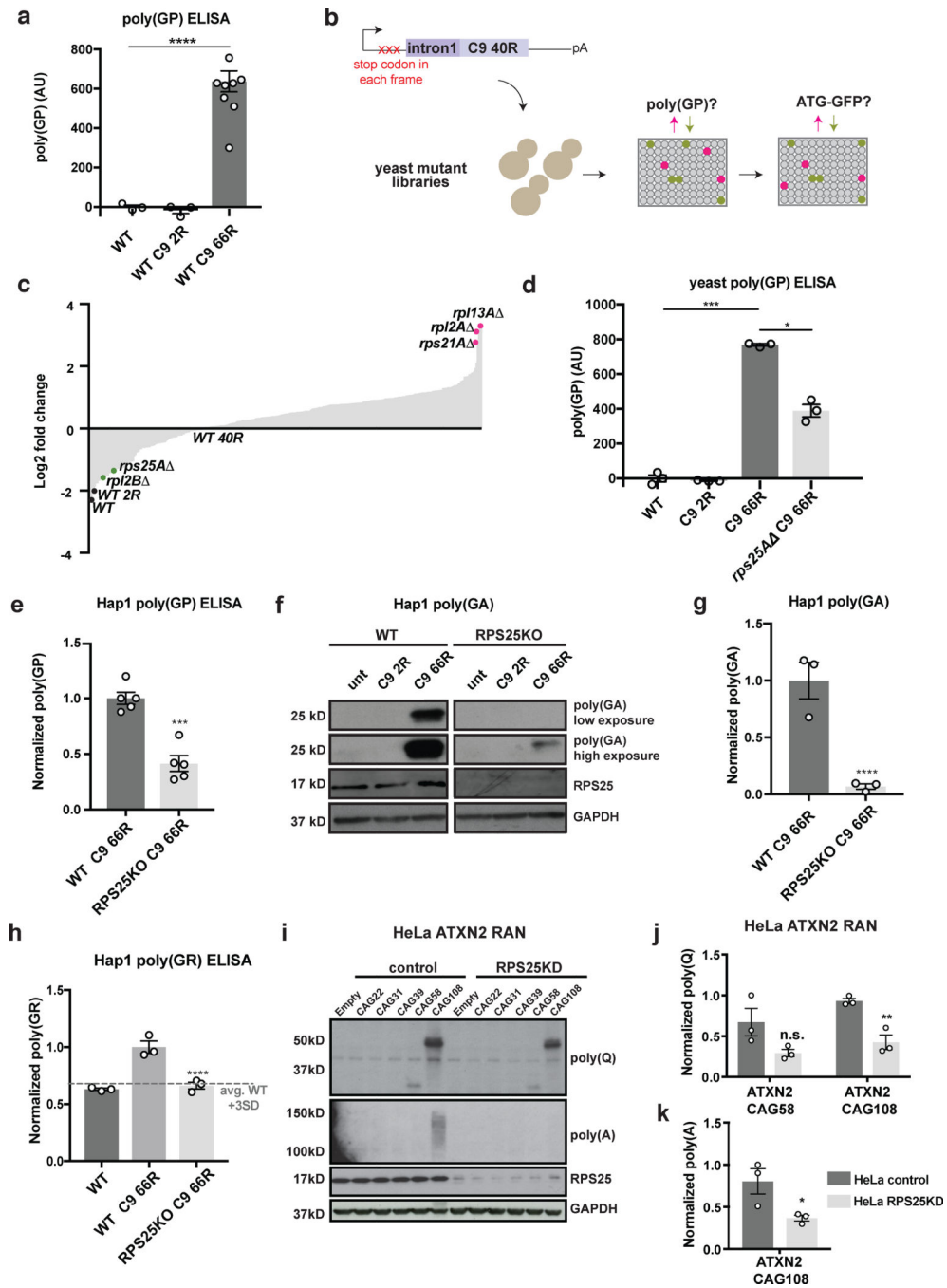


Figure 1: RPS25 is required for efficient RAN translation in yeast and human cells.

(a) Detection of RAN-translated DPR in yeast lysate using a poly(GP) immunoassay. Wildtype (BY4741) yeast were transformed with an empty vector or constructs expressing either 2 or 66 *C9orf72* GGGGCC repeats (C9 2R or 66R) under the control of a galactose inducible promoter. DPR production was assayed in yeast lysates using a poly(GP) immunoassay. We detected poly(GP) in the C9 66R expressing yeast (two-tailed, unpaired t-test; n=3 WT and WT C9 2R transformations; n=8 independent *rps25A* C9 66R transformations; ****p<0.0001; mean +/- s.e.m.). (b) Schematic of yeast poly(GP) and

ATG-GFP counter screen to identify RAN translation regulators. C9 40R expression constructs were introduced by transformation or mating into yeast mutants from the deletion collection (MATa; non-essential genes) and DAmP library (essential genes). Mutants were assayed for poly(GP) levels using a poly(GP) immunoassay and counter-screened with a GFP immunoassay. Data provided in Table S1. (c) Fold-change poly(GP)-levels of yeast mutants compared to wildtype yeast expression is shown (n=3 independent transformations for each strain). (d) Independent validation of *rps25A* mutant expressing C9 66R using poly(GP) immunoassay. Poly(GP) levels were approximately 50% lower in *rps25A* compared to wildtype yeast (two-tailed, unpaired t-test; n=3 independent deletion strains; ***p=0.0010, *p=0.0248; mean +/- s.e.m.). (e) Immunoassay shows RPS25KO in the human Hap1 cell line reduces poly(GP) levels (two-tailed, unpaired t-test; n=5 independent cell culture experiments; ***p=0.0002; mean +/- s.e.m.). (f) Lysates from transfected Hap1 cells were immunoblotted for poly(GA) expression (HA-epitope tag). (g) Quantification of (f) (uncropped blots for this and all subsequent blots can be found in Supplemental Fig. 11; two-tailed, unpaired t-test; n=3 independent cell culture experiments; ****p<0.0001; mean +/- s.e.m.). (h) Immunoassay shows RPS25KO in Hap1 cells reduces poly(GR) levels to that of Hap1 wildtype transfected with empty vector. Full conditions and ANOVA statistics shown in Fig. S3 (ordinary one-way ANOVA with Tukey's multiple comparisons, n=3 independent cell culture experiments; ****p<0.0001; mean +/- s.e.m.). (i) Lysates from transfected HeLa cells were immunoblotted for poly(Q) and poly(A) *ATXN2* RAN products. (j and k) Quantification of (i) where poly(Q) or poly(A) are normalized to GAPDH. (j) *ATXN2* CAG108 RAN translated poly(Q) products are reduced in HeLa cells harboring a CRISPR-induced mutation that markedly reduces level of RPS25 (RPS25KD) compared to HeLa control cell (two-tailed, unpaired t-test; n=3 independent cell culture experiments; **p=0.0059, n.s., not significant p=0.0946; mean +/- s.e.m.). (k) *ATXN2* CAG108 RAN poly(A) products are reduced in HeLa RPS25KD mutant compared to HeLa control (two-tailed, unpaired t-test; n=3 independent cell culture experiments; *p=0.0473; mean +/- s.e.m.). Additional statistical details for this figure and subsequent figures are provided in **Table S4** and the **Methods**.

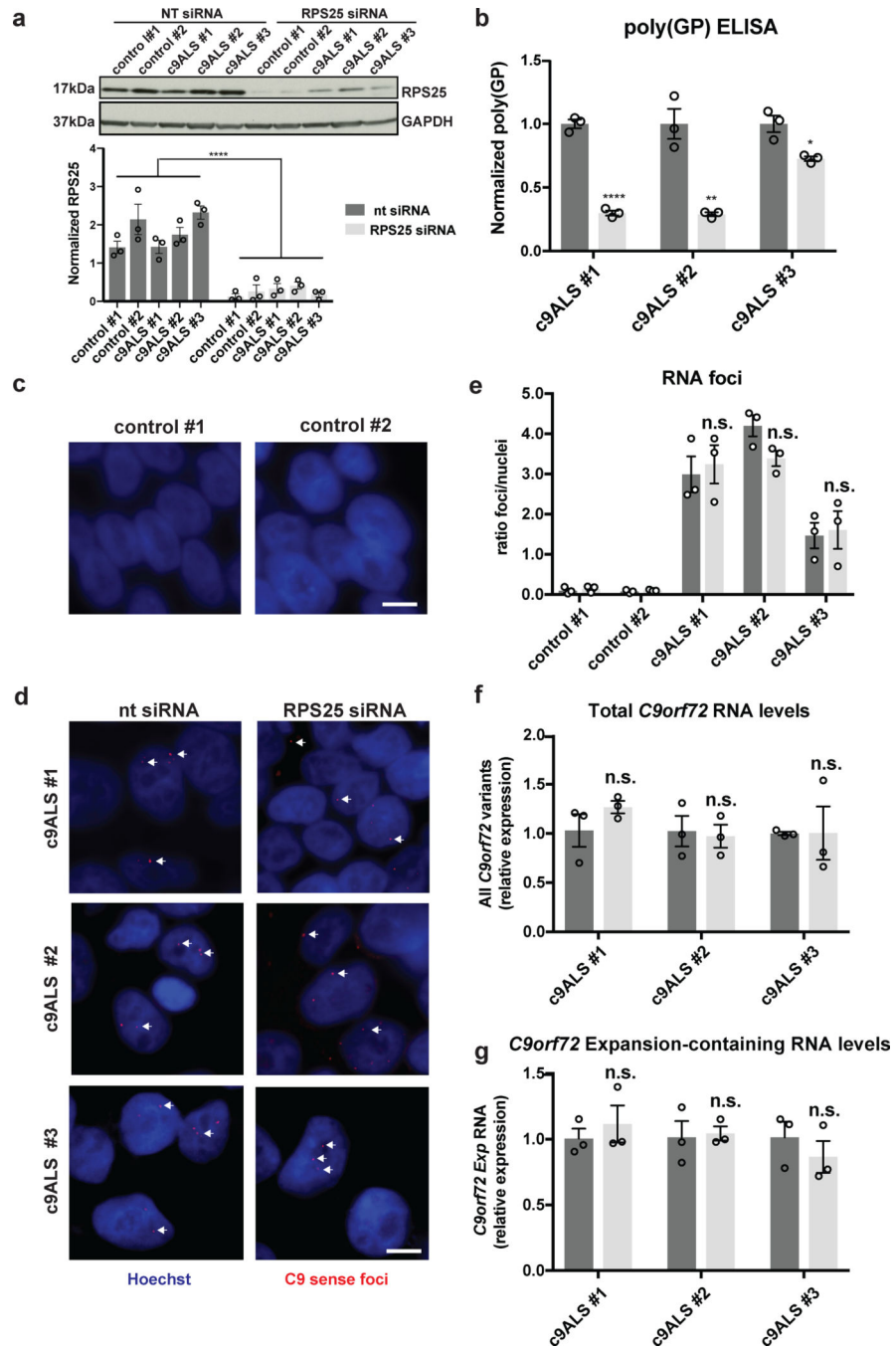


Figure 2: RPS25 knockdown reduces poly(GP) levels in *C9orf72* ALS patient iPSCs. Control and c9ALS patient-derived iPSCs were treated with non-targeting control siRNA or RPS25-targeting siRNA. **(a)** Lysates from iPSCs treated with non-targeting or RPS25-targeting siRNAs were immunoblotted for RPS25 expression. Quantification illustrates that RPS25 is reduced in RPS25-targeting siRNAs (One-way ANOVA with Tukey’s multiple comparisons, n=3 independent cell culture experiments per iPSC line and condition; ****p<0.0001; mean +/- s.e.m.). **(b)** Immunoassay for poly(GP) levels in c9ALS iPSCs shows reduction of poly(GP) levels in RPS25 siRNA-treated cells (two-tailed, unpaired t-

test; n=3 independent cell culture experiments per iPSC line and condition; ****p<0.0001, **p=0.0039, *p=0.0161; mean \pm s.e.m.). See also Fig. S5B. **(c and d)** RNA FISH with probe for GGGGCC (sense) RNA was used to detect and quantify sense repeat foci, pseudocolored in red. Cell nuclei are indicated in blue (Hoechst 33258). Scale bar: 5 μ m. **(c)** Control iPSCs derived from healthy subjects. **(d)** c9ALS-patient derived iPSCs. **(e)** Quantification of normalized foci per nuclei (two-tailed, unpaired t-test; n=3 independent cell culture experiments; n.s., not significant, (c9ALS #1) p=0.7234, (c9ALS #2) p=0.0654, (c9ALS #3) p=0.8189; mean \pm s.e.m.). **(f)** RT-qPCR of total *C9orf72* mRNA (two-tailed, unpaired t-test; n=3 independent cell culture experiments; n.s., not significant, (c9ALS #1) p=0.2509, (c9ALS #2) p=0.8068, (c9ALS #3) p=0.9912; mean \pm s.e.m.). **(g)** RT-qPCR of *C9orf72* mRNA variants harboring the repeat expansion (two-tailed, unpaired t-test; n=3 independent cell culture experiments; n.s., not significant; (c9ALS #1) p=0.5289, (c9ALS #2) p=0.8390, (c9ALS #3) p=0.4279; mean \pm s.e.m.).

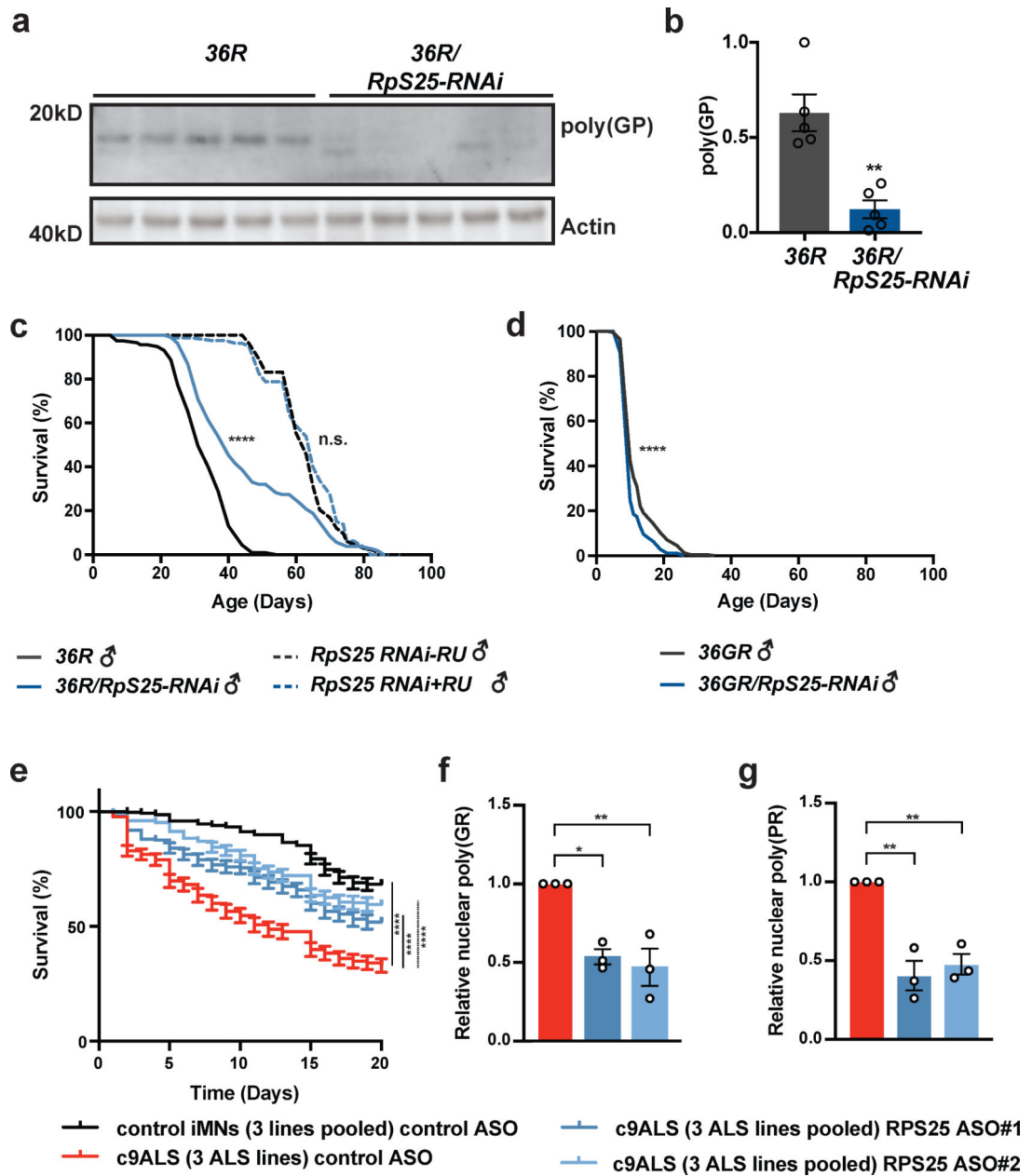


Figure 3: RPS25 knockdown reduces RAN translation products and extends lifespan in a *Drosophila C9orf72* model.

(a) Immunoblot of fly heads expressing 36(GGGGCC) (36R) alone or together with RpS25 RNAi in adult neurons, showing a reduction of poly(GP) levels in 36R flies expressing RpS25 RNAi. Genotypes: *UAS-36(GGGGCC)/+; elavGS*, *UAS-36(GGGGCC)/RpS25RNAi {KK107958}; elavGS/+*. (b) Quantification of blots in (a) (two-tailed, unpaired t-test; n=5 biological replicates; **p=0.0015). (c) Survival curves of male flies expressing an inducible 36(GGGGCC) construct alone or together with RpS25 RNAi. RpS25 RNAi resulted in a lifespan increase in the 36R flies (chi-squared log-rank test; ****p<0.0001). Median lifespans: C9 36R flies, 29 days; C9 36R/RpS25-RNAi, 38 days. Genotypes and n: *UAS-36(GGGGCC)/+; elavGS* (n=115 flies), *UAS-36(GGGGCC)/*

RpS25RNAi{KK107958}; elavGS/+ (n=106 flies)). In separate analyses, flies expressing RpS25 RNAi alone did not alter lifespan (chi-squared log-rank test; n=83 uninduced, n=80 RNAi induced; n.s., not significant p=0.4766). Median lifespans: RpS25-RNAi uninduced, 59 days; RpS25-RNAi induced, 61 days. Genotype: UAS-RpS25RNAi{KK107958}/+; elavGS/+). (d) Expression of RpS25 RNAi together with AUG-driven codon-optimized 36 Glycine-Arginine repeats (36GR) decreases survival of male flies (chi-squared log-rank test; ****p<0.0001). Genotypes: UAS-36GR/+; elavGS (n=226 flies), UAS-36GR/RpS25RNAi{KK107958i}; elavGS/+ (n=180 flies). 36R flies are codon optimized, driven by AUG and do not undergo RAN translation. (e) Quantification of surviving induced motor neurons (iMNs) derived from a c9ALS iPSC line #4–6 and 3 control iPSC lines treated with RPS25-targeting antisense oligonucleotides (ASO1 and 2) or control ASO control. The survival of HB9-RFP+ iMNs was tracked by imaging after addition of 10µM glutamate. Treatment of RPS25 ASO1 and ASO2 significantly increased survival of 3 c9ALS iMN lines ((log-rank tests; n=3 independent iMN lines per condition per treatment; ****p<0.0001; error bars, s.e.m.). (f) Relative nuclear poly(GR) quantification 3 c9ALS iMN lines treated with control or RPS25-targeting ASOs (one-way ANOVA with Tukey's multiple comparison; n=3 independent iMN lines per condition per treatment with 20 iMNs analyzed and averaged for each n; **p=0.0055, *p=0.0105; mean +/- s.e.m.). (g) Relative nuclear poly(PR) quantification 3 c9ALS iMN lines treated with control or RPS25-targeting ASOs (one-way ANOVA with Tukey's multiple comparison; n=3 independent iMN lines per condition per treatment with 20 iMNs analyzed and averaged for each n; (ASO1) **p=0.0017, (ASO2) **p=0.0034; mean +/- s.e.m.). For (f) and (g), individual data per c9ALS iMN line can be found in Fig. S8 and representative immunocytochemistry can be found in Fig. S10.